Acta Cryst. (1996). B52, 165–183

Predicting the Crystal Structure of Organic Molecular Materials

ANNE M. CHAKA,† REBECCA ZANIEWSKI, WILEY YOUNGS,‡ CLAIRE TESSIER‡ AND GILLES KLOPMAN*

Department of Chemistry, Case Western Reserve University, Cleveland, Ohio 44106, USA

(Received 17 March 1994; accepted 23 May 1995)

Abstract

This paper describes a novel method for predicting the crystal structure of organic molecular materials which employs a series of successive approximations to focus on structures of high probability, without resorting to a brute force search and energy minimization of all possible structures. The problem of multiple local minima is overcome by assuming that the crystal structure is closely packed, thereby eliminating 217 of the 230 possible space groups. Configurations within the 13 remaining space groups are searched by rotating the reference molecule about Cartesian axes in rotational increments of 15°. Initial energy minimization is performed using (6–12) Lennard–Jones pair potentials to produce a set of closely packed structures. The structures are then refined with the introduction of a Coulombic potential calculated using molecular multipole moments. This method has successfully located local minima which correspond to the observed crystal structures of several saturated and unsaturated hydrocarbons with no *a priori* information provided. For large polycyclic aromatic hydrocarbons, additional refinements of the energy calculations are required to distinguish the experimental structure from a small number of closely packed structures. Our methodology for *a priori* crystal structure prediction represents the most efficient algorithm presented to date, in a field where the first successes have only been described within the past year and have been few and far between. Since our algorithm is capable of locating a large number of reasonable structures with similar energy in a short period of time, and is more likely to locate a minimum corresponding to the experimental structure, our program provides a superior framework to determine the level of theory required to calculate the intermolecular potential. For all but highly asymmetric hydrocarbons, however, distinguishing the observed structure from a large number of highly probable structures requires more rigorously calculated intermolecular interactions than pair potentials, plus an *ad hoc* electrostatic potential, and is thus beyond the scope of this paper. All calculations were performed on the Ohio Supercomputer Center's Cray Y-MP.

1. Introduction

Considerable interest has developed in organic molecular materials, thin films and monolayers (Roberts, 1983; Sugi, 1985) since the discovery of a wide range of properties previously thought to be the exclusive domain of inorganic materials and metals. Many of these electronic (Hoffman, Marinsen, Pace & Ibers, 1983), magnetic (Miller, Epstein & Reiff, 1983) and optical properties (Williams, 1984; Chemla & Zyss, 1987) are dependent upon the relative orientation of the constituent molecules within the material. Organic materials have an advantage over more traditional materials in that their properties can be tailored to a specific application by changing the structure of the constituent molecules. Important differences in the magnitudes of various properties can be achieved by subtle modifications of the functional groups on a given molecule. In addition, organic materials can be designed which exhibit these properties anisotropically.

Most of these properties are dependent upon the relative orientation of the molecules within the material, *i.e.* how the molecules are packed within the crystal. In the field of optics, for example, materials must crystallize in a noncentrosymmetric space group to exhibit second-order nonlinear optical characteristics (Chemla & Zyss, 1987), which are important in applications involving optical circuits and information transmission. While inorganic materials are often easily made, however, the synthesis of organic molecules is often quite difficult and time consuming. Hence, there is a need to improve our understanding of how these materials crystallize in order to provide some direction to the synthetic chemist. Unfortunately, there is no working method yet available which is able to predict *a priori* whether a molecule to be synthesized will crystallize in a particular space group and hence be more likely to express the desired properties macroscopically in the bulk phase. The few successes which have occurred (Taylor & Kennard, 1984; Gavezzotti & Desiraju, 1988; Gavezzotti, 1989, 1990, 1991; Karfunkel & Gdanitz, 1992; Holden, Du & Ammon, 1993) have come only recently and have had limited applicability due to computational

† Current address: The Lubrizol Corporation, 29400 Lakeland Blvd, Wickcliffe, Ohio 44092, USA.

‡ Current address: Department of Chemistry, University of Akron, Akron, Ohio, USA.

limitations and inadequate intermolecular potentials. We have developed a method which provides a more thorough and efficient evaluation of the search space than those previously published. The generation of a large number of reasonable structures with a small investment in c.p.u. time provides a framework for the evaluation of intermolecular potentials and has allowed us to develop a guide for the level of theory required to calculate the nonbonded interaction energy for certain types of molecules. We have shown that pair potentials plus any type of *ad hoc* electrostatic potential are adequate for only irregularly shaped molecules and are not sufficient to distinguish the observed structure from a myriad of other closely packed structures at this level of refinement. There are systems, such as planar aromatic hydrocarbons, which will probably require calculations at the highest levels of theory.

We limit our study to molecular materials in which there is no charge transfer and the dominant cohesive force of the lattice is due to weak van der Waals interactions.

2. Progress in the field to date

To be able to predict crystal packing has long been recognized as being of great importance, but was believed to be too complicated and to involve too many long calculations to be feasible. The observed structure would, of course, be the lowest energy configuration possible. Unfortunately nonbonded interactions, which are responsible for the cohesion of molecular solids, are difficult to quantify. Semiempirical methods are very fast, but errors due to the exclusion of explicit correlation effects and the use of a minimal basis set are often greater than the magnitude of the energy of the van der Waals interaction, making them inappropriate for nonbonded solids. The *ab initio* calculation of nonbonded species using post-Hartree–Fock methods requires extensive basis sets, configuration interaction and inclusion of correlation effects, and can therefore be performed only on small molecules (Buckingham & Fowler, 1983, 1985; Jeziorski, Moszynski & Szalewicz, 1994; Rybak, Jeziorski & Szalewicz, 1991; Rybak, Szalewicz, Jeziorski & Jaszunski, 1987; Stone, 1981; Szalewicz & Jeziorski, 1979). One approach to predicting crystal structure has been to use highly accurate *ab initio* calculations on a small molecular cluster – usually a dimer. Due to computational limitations, however, performing geometry optimizations on any system larger than the benzene dimer is not practical for routine investigations or predictions. Nor can these dimer calculations model the packing effects of other molecules in an infinite lattice.

Several methods based on density functional theory, although faster than the Hartree–Fock-based methods, are also too computationally intensive with periodic boundary conditions to optimize the geometry of a large number of possible crystal structures and perform an exhaustive search of multiple local minima. In addition, these methods, which require nonlocal corrections to the exchange and correlation to treat nonbonded interactions, have not been extensively applied to crystal structures of sizeable organic molecules.

In view of the computational requirements necessary to accurately calculate nonbonded interactions using quantum mechanics, the energy is usually approximated using empirical van der Waals pair potentials plus some form of *ad hoc* electrostatic potential. Even with a simplified form of the potential, however, prediction techniques based on lattice energy minimization alone are not practical for molecular solids. The principal difficulties are due to the number of multiple minima in a very large search space and the extensive computation time required to evaluate energy gradients over several unit cells, particularly if a $1/r$ term is used in the electrostatic potential.

Before much computational power was available, structure predictions relied on making analogies with similar molecules of known crystal structure. Unfortunately, molecules with very similar structures can crystallize in very different orientations and the usefulness of the structural analogy approach has been limited. For example, benzene crystallizes in a herringbone configuration with four molecules per unit cell (Cox, Cruickshank & Smith, 1958; Bacon, Curry & Wilson, 1964), hexachlorobenzene in a face-to-face stacked arrangement with two molecules per cell (Bondi, 1968) and hexafluorobenzene in a different herringbone configuration with six molecules per unit cell (Boden, Davis, Stam & Wesselink, 1973). More recently, Gavezzotti & Desiraju (1988) have had some success in correlating the molecular geometry of fused-ring aromatic hydrocarbons with the type of closely packed clusters observed within different crystalline polymorphs, despite different space-group symmetries. Gavezzoti and others have also had some limited success correlating various structural and electrostatic descriptors with crystal structures, but the reliability of these calculations has been erratic because correlations were not observed in all cases (Gavezzotti & Desiraju, 1988; Gavezzotti, 1989, 1990; Taylor & Kennard, 1984). Unfortunately, no effective general method based on structural analogies has yet been developed.

Another approach to predicting the crystal structure of molecular solids has been to model the process of crystallization using cluster calculations. Williams (1980), van de Waal (1981) and Oikawa, Tsuda, Kato & Urabe (1985) have performed cluster calculations on benzene as a model compound using potentials with point charges on the atoms to account for the polarization across the C—H bond. In all cases, the tendency of benzene to pack edge-to-face was apparent in the clusters, but intermolecular distances and angles differed markedly from those observed in the solid state. In order

to obtain quantitative agreement with experimental crystal structure, Oikawa, Tsuda, Kato & Urabe (1985) concluded that cluster calculations of 168 molecules, arranged in layers in 16, 36, 64, 36 and 16 molecules, would be necessary. They were unable to perform these calculations on larger clusters due to economic and computational limitations. Another difficulty with cluster calculations arises in that the minimum energy configuration obtained in a cluster calculation may not exhibit the translational invariance consistent with the crystal lattice. Hence, whereas cluster calculations can be useful for obtaining qualitative information about the crystal packing of small, symmetric molecules such as benzene, the large number of degrees of freedom and consequent computational requirements make them impractical for larger, asymmetric molecules.

Recent work by Gavezzotti (1991) has circumvented some of the problems inherent in cluster calculations and, in a few special cases, has been able to predict the observed crystal structure on the basis of molecular structure alone. Gavezzotti eliminated a few degrees of freedom by constraining two to four molecules to move, consistent with the most commonly observed symmetry elements: the inversion center, the screw axis and the glide plane. The most promising small nuclei of molecules thus obtained are then selected on the basis of a statistical analysis of known structures, as well as subjective judgement by the user, for translational searches with full crystal symmetry. In many cases the space-group symmetry was imposed by the user. This method is very time consuming, requiring a full day to search even one space group on a Gould-NP1 mini-supercomputer. Although Gavezzotti's combination of cluster minimization, statistical analysis and user judgement represents a significant contribution to a field 'where anything above zero is considered a good percentage of success', the method was not able to locate a minimum corresponding to the experimental structure for the majority of the 20 examples cited. This failure to locate the observed minimum indicates that this method does not adequately sample the search space. Unfortunately, the necessity of subjective judgement by the user, as well as computational requirements and insufficient sampling of possible configurations, represents a real limitation of this technique as a widely applicable general method.

Most of the modeling of organic molecular crystal lattices, as opposed to clusters, has been developed to aid in locating molecules in the unit cell from diffraction data and to check the plausibility of X-ray structural refinements (Williams, 1969). Williams (1983), who carried out the first work in this area, developed a program to optimize the molecular orientation within an assumed space group by minimizing the lattice energy based on experimentally determined parameters. However, if the input deviates slightly from the actual values, the calculation can easily become trapped in a local minimum and give a misleading result. In addition, we have determined that if the crystal structure is initially expanded to a point where the molecules are free to rotate, Williams' program *PCK*83 is then unable to contract the lattice to find a stable minimum. To obtain a useful structure prediction using *PCK*83, one must already know, to within a high degree of certainty, what that structure already is, as in X-ray diffraction structural refinements.

The first predictive method which does not rely on experimental data which has had some success is a Metropolis (Rosenbluth, Rosenbluth, Teller & Teller, 1953) Monte-Carlo-simulated annealing technique (Kirkpatrick, Gelatt & Vecchi, 1983) employed by Gdanitz (1992). The technique was successful for some molecules with very simple crystal structures in space groups $P1$, $P\bar{1}$ or $P2$ with $Z = 1$ or $Z = 2$, but not with all. For several molecules, such as 3,6-dimethylenepiperazine-2,5-dione (Karfunkel & Gdantiz, 1992), the method did not locate minima corresponding to experimental structures for all compounds tested due to prohibitive c.p.u. time consumption. This method does not differ significantly from the cluster calculational methods discussed previously, except that periodic boundary conditions are maintained by placing 26 identical clusters around the reference cluster. There are no symmetry constraints employed within the cluster calculation. With molecules which exhibit more complex crystal packing, however, it has yet to be demonstrated that this Monte-Carlo-simulated annealing technique will be sufficient to overcome the computational limitations due to too many local minima and too many degrees of freedom which has plagued other Monte Carlo cluster methodologies which do not employ symmetry restrictions and periodic boundary conditions.

A recently developed program at the University of Maryland, *MOLPAK*, has successfully predicted structures of C-, H-, N-, O- and F-containing compounds in the primitive triclinic, monoclinic and orthorhombic space groups with $Z \leq 4$ (Holden, Du & Ammon, 1993). In *MOLPAK* molecules are initially packed along an axis by varying the Eulerian angles and intermolecular distances. The closely packed axes are then arranged into two-dimensional arrays and lastly the two-dimensional layers into three-dimensional arrays, using a repulsive-only potential. The principal acceptance criteria for a given orientation within a space group is minimum volume. The crude packing arrangements are then refined using the *WMIN* program. *MOLPAK* is currently limited to four space groups, $P\bar{1}$, $P2_1$, $P2_1/c$ and $P2_12_12_1$. Holden, Du & Ammon (1993) obtained good results for nitro compounds, locating minima similar to experiment in at least 10 out of 14 compounds. Discrepancies with experimentally observed structures were attributed to inadequacies of the *WMIN* forcefield. This approach of packing molecules first in one, then two and finally three dimensions is similar to the cluster

building approach of Gavezzotti. It is not clear, however, whether this approach would work for molecules which may not form closely packed axes, yet are closely packed in three dimensions. Benzene, which crystallizes in an edge-to-face geometry, may be an example of such a molecule. In addition, our results have shown that a 6–12 potential is faster than a repulsive-only potential and is a more reliable initial prediction criterium than minimum volume (see §5 and 8, particularly the results for durene).

3. Methodology

We have developed an approach to predicting the crystal structures of organic molecular materials which circumvents the difficulties of multiple local minima, and the extensive computation time required to evaluate energy gradients over several unit cells, by using a series of successive approximations to focus on crystal structures of high probability without user intervention or performing a search by brute force of the almost infinite number of possibilities. Our program *ICE*9 is very efficient and highly vectorized, enabling us to make crystal structure predictions of large molecules in less than 2 h c.p.u. time on a Cray Y-MP.

The vast majority of organic compounds crystallize into regular arrays in the solid. Amorphous materials are rare. Hence, the first assumption we make in our refinement process is that the solid will be crystalline and during the energy minimization process the molecules are constrained to move in accordance with specific symmetry operations, thus eliminating translational and rotational degrees of freedom for all but the reference molecule. The maximum number of variables in the energy minimization process is 12: three rotational and three translational degrees of freedom for the reference molecule, the magnitude of each of the three lattice vectors and the three lattice angles. This maximum of 12 variables is in stark contrast to the $6(N-1)$ variables required in the cluster calculations of N molecules performed by Williams, van de Waal, Oikawa and others.

Imposing the condition of crystallinity on the structure of the molecular solid reduces the number of possible configurations from infinity to a finite number within the 230 space groups. Unfortunately, within each space group there are still many orientational degrees of freedom possible consistent with a given set of symmetry constraints. We estimate that a reasonably fine search mesh for a large asymmetric molecule in a given space group consists of 10^6 orientations. If there is more than one molecule in the asymmetric unit, the number of possibilities is increased by several orders of magnitude. Therefore, searching all 230 space groups is not practical.

Fortunately, the 230 possible space groups are not observed with equal frequency. In most of the space groups certain symmetry features, such as mirror planes and rotation axes, create large gaps or holes in the crystal structure when filled with irregularly shaped molecules. In the 1950's, Kitaigorodsky (1973) performed a systematic study of the symmetry of organic molecular solids and determined that close-packing of organic molecules is possible in only 13 of the 230 space groups. Kitaigorodsky's hypothesis has been verified experimentally. Of 29059 organic compounds whose crystal structures were determined prior to 1981, 75% crystallized in only five space groups (Mighell, Himes & Rodgers, 1983). These five space groups exhibit combinations of inversion centers, screw axes and/or glide planes which facilitate close-packing in all three lattice directions. For totally asymmetric molecules, close-packing is possible only in the following space groups: $P\bar{1}$, $P2_1$, $P2_1/c$, $Pca2_1$, $Pna2_1$ and $P2_12_12_1$. For centrosymmetric molecules the possibilities are even fewer: $P\bar{1}$, $P2_1/c$ and $Pbca$.

Reducing the number of possible space groups from 230 to 13 is the next major step in the refinement process for predicting crystal structures. Hence, we not only limit our search by constraining molecules to move in a symmetrical manner during the energy minimization process, but we only allow those symmetry elements which give us the highest probability of obtaining a closely packed structure.

3.1. *Close-packing the crystal structure*

The 13 most probable space groups must be searched systematically for the lowest energy configurations. Fortunately, in organic molecular materials, the molecule maintains its integrity in the solid state, *i.e.* the structure the molecule exhibits in the gas phase is fairly well retained in the solid state, with distortions being minor, if present at all (Kitaigorodsky, 1973). Hence, for this initial version of the program we maintain the molecular structure in a rigid conformation. Even with the variables of molecular flexibility eliminated, the search space is still too large to use the most sophisticated methods available to calculate the intermolecular interactions and minimize the energy, and hence the following assumptions are made to simplify the calculation at this stage of refinement:

(1) The crystal structure will be closely packed.

(2) The molecules are assumed to be completely dielectric, *i.e.* no charge transfer occurs.

(3) Coulombic interactions beyond van de Waals are ignored.

(4) Thermal effects are ignored.

(5) Not many body effects are considered.

(6) The molecule is rigid and will exist in its optimized gas-phase conformation.

van de Waals pair potentials can be used effectively to describe the shape of the molecule for the close-packing portion of the program. We have found the Lennard–Jones form (6–12) to be at least an order of magnitude faster to calculate than either the Buckingham (exp-6) form or a simple hard-sphere packing approach. The

Lennard–Jones expression used is of the following form

$$E_{ij} = 4\varepsilon_{ij}\left[(\sigma_{ij}/r_{ij})^{12} - (\sigma_{ij}/r_{ij})^{6}\right], \quad (1)$$

between two atoms i and j separated by the distance r_{ij}, where ε_{ij} is the depth of the potential well and σ_{ij} is the internuclear separation for which the interaction energy is zero. To obtain Lennard–Jones parameters for our work, we fit the σ and ε shown in (1) to the lowest temperature structures available for the aromatic hydrocarbons benzene (Bacon, Curry & Wilson, 1964), naphthalene (Kozin & Kitaigorodsky, 1953) and anthracene (Mason, 1964). The parameters were varied to obtain a least-squares fit to the lattice constants when used in *ICE*9. The values of σ_i and ε_i for carbon are 1.694 Å and 0.7266 $(\text{kJ mol}^{-1})^{1/2}$, and 1.272 Å and 0.7108 $(\text{kJ mol}^{-1})^{1/2}$ for hydrogen. The σ_{ij} and ε_{ij} terms in (1) are the sum and product of the individual ij's, respectively. Our 6–12 potential curve for hydrocarbons is very similar to that obtained using the exp-6 form with Williams' parameters (Williams & Starr, 1977).

The main obstacle to finding an absolute minimum is the barrier of molecular rotation between local minima. The various space groups have different numbers of parameters which can vary and hence have different likelihoods of multiple minima. For a given space group, the greater the number of variable lattice dimensions and angles, the higher the likelihood that a large number of multiple minima exists. The number of rotations of trial starting positions required to generate a complete search space is dependent upon the molecular symmetry. Our work, as well as that of Williams (1969) and Price (1986), indicates that for even the very worst case of an asymmetric molecule, successive runs with initial molecular positions rotated in increments of 15° result in a relatively thorough search of possible configurations in a space group. Space groups which do not allow close-packing can be readily eliminated at this point without a more extensive search. Molecules with low symmetry or a large number of protrusions, however, can require smaller rotational increments to ensure a complete search space in the remaining space groups which facilitate the closest packing.

The higher the symmetry, or the fewer the number of protrusions on the molecule, the fewer the rotation increments required.

4. Details of the program *ICE*9

The only input required for *ICE*9 is the molecular geometry, multipole moments and van der Waals volume. In this work optimized geometries of the molecules were obtained from *Gaussian*88 and *Gaussian*90 (Frisch *et al.*, 1990) using a 3-21G basis set. The calculated geometries were found to be consistent with the experimental structures. *ICE*9 does not perform any optimization or internal geometry modifications of the molecule or asymmetric unit provided in the input file. Molecular multipole moments were calculated with *Gaussian*90 using a 6-31G* basis set. The van der Waals volumes were calculated from *CHEM-X*, which uses van der Waals' radii of 1.0 Å for hydrogen and 1.6 Å for carbon (*CHEM-X*, 1990). The *CHEM-X* van der Waals' radii are slightly smaller than the 1.1 and 1.8 Å radii typically observed in hydrocarbon crystal structures. Hence, the calculated packing indices are systematically smaller than those usually reported, but the relative values are consistent and can be used for comparison.

In the program the molecular point group is determined automatically and the molecule is positioned with its center of mass at the origin, and the principal axes of inertia are aligned with the Cartesian axes. The molecule is then rotated a certain number of degrees about the x, y or z axes. The default rotation increment is 15° to ensure a relatively complete search and eliminate unfavorable space groups. A finer rotational grid can then be employed as an additional refinement on the remaining space groups which facilitate close-packing. The limits of the initial rotations are determined automatically by the molecular point group to eliminate redundant starting configurations for highly symmetric molecules. For a molecule such as benzene, approximately 2600 starting positions, distributed over 13 space groups, are used. Once the molecule is rotated about the origin, the reference unit cell is constructed around it. The magnitudes of the lattice vectors **a**, **b** and **c** are initially set to 2.5 times the maximum van der Waals diameter of the molecule. For space groups in which general positions are occupied, the molecule is translated to a central general position at (0.25**a**, 0.25**b**, 0.25**c**). For a space group in which special positions are occupied, the molecule is placed directly on the special position.

Once the unit cell is constructed, it must be placed in the crystal environment. The most direct way is to construct 26 unit cells in a $3 \times 3 \times 3$ array around the reference unit cell. This is fairly time consuming, however, and a much more efficient yet effective method for fairly compact molecules is to construct a $2 \times 2 \times 2$ arrangement of unit cells and simply shift the reference cell. To prevent overlap between molecules more than one unit cell apart, which can occur during minimization when a lattice constant can become much smaller than the length of an extended molecule, the centers of mass of all the molecules in a $5 \times 5 \times 5$ array of unit cells are calculated. Atomic coordinates and interaction energies are then calculated only for those molecules whose centers of mass are separated from the reference molecule by less than the maximum molecular diameter plus the minimum van der Waals' radius. In addition, the interaction energy between the reference molecule and the molecules in the [1,1,1] unit cell are always calculated to facilitate the minimization process in the early stages when no molecules outside the reference unit cells may lie within the cutoff radius. This may be the

reason Williams' *PCK*83 does not converge for sufficiently expanded unit cells.

4.1. *Optimization of variables*

Once the block of unit cells is constructed with the proper space-group symmetry, the structure of the crystal is minimized with respect to all or part of the following variables: rotation and translation of the asymmetric unit, the magnitude of the lattice vectors and the three lattice angles. For the energy minimization, only the atomic coordinates and the pairwise interaction energy between atoms in molecules are calculated whose centers of mass are separated by less than the maximum van der Waals diameter. The time required to minimize the energy of a triclinic crystal structure, with 12 variables, two benzene molecules per unit cell and 12 atoms per molecule, is approximately 490 ms on a Cray Y-MP. An orthorhombic structure with six variables to optimize and four benzene molecules per unit cell requires 110 ms. Performance on a single processor on the OSC Cray Y-MP ranged between 185 and 245 MFLOPS sustained, depending on the number of atoms per molecule which in turn determines the vector length.

4.2. *Sorting close-packed structures*

The 2–10 000 closely packed structures obtained from the minimization process are then sorted to produce a list of the most probable structures. At this stage the Lennard–Jones energy is recalculated with a 10 Å cutoff radius to improve the reliability of the selection process, as opposed to just the nearest neighbor interactions used during the minimization procedure. For saturated hydrocarbons or irregularly shaped molecules, sorting on the basis of a converged Lennard–Jones energy is sufficient for a good structure prediction. For molecules with any degree of polarity, however, electrostatic interactions are a necessary additional refinement for the energy calculation used to sort the close-packed structures (Williams, 1974; Hall & Williams, 1975; Williams & Starr, 1977), although they are not necessary to obtain the closely packed structures themselves. Without the additional electrostatic potential, the edge-to-face packing of benzene, for example, would be predicted to be lower in energy than the observed slipped-stack configuration. Shi & Bartell (1988) have shown, using the 12-point charge model for the charge distribution in benzene, the effect of varying the magnitude of the point charge q on the shift from the observed equilibrium Eulerian angles of the reference molecule in crystalline benzene. The experimentally observed quadrupole moment of benzene is reproduced by point charges of magnitude ± 0.153 located at the nuclei. For values of q ranging from 0.125 to 0.175, the Eulerian angle shifts by only $\pm 1°$, and for q from 0.1 to 0.15, by only $\pm 3°$. Below a value of 0.09 for q, however, dramatic changes in Eulerian angles from 12° to more than 20° were observed.

Various methods of calculating the electrostatic energy were evaluated to determine which, if any, were fast enough to be performed on every close-packed structure before the final predictions are made. The electrostatic potential of a molecule is a rigorously defined property which can, in principle, be calculated exactly from the molecular wavefunctions. Realistically, however, it is not possible at the present time to calculate the electrostatic energy exactly from *ab initio* wavefunctions for a molecular solid, and therefore approximations must be used. There are four types of models which can be used to approximate the molecular charge distribution. In one model the charge distribution is considered as a group of discrete point charges usually, but not necessarily, located at the atomic nuclei. This is the most common method used for nonbonded interactions. Another approach, very similar to the point charge method, is the bond or group dipole model in which the electron distribution is described by point dipoles located in bonds between the atoms in the molecule. Third, the charge distribution is described by multipole expansions about atomic centers. Lastly, the charge distribution of the molecule is expressed in a molecular multipole expansion.

Each method of approximating the electrostatic interactions was examined with respect to accuracy and efficiency. Only the molecular multipole model, although the crudest approximation to the molecular charge distribution, was found to be fast enough to be calculated for every close-packed structure in the final sorting process and yet yield reasonable agreement with more accurate methods. The molecular multipole model is most inappropriate for cases in which the charge distribution of one molecule significantly penetrates that of its nearest neighbor, but it does yield good results for the electrostatic energy when the charge distributions are separate (Jackson, 1962). To calculate the energy between two charge distributions, a and b, it is convenient to express their orientation in a coordinate system in which their z-axes are coincident and the x and y axes are parallel. If these charge distributions do not overlap, the potential energy between them can be expressed as

$$\varphi_{ab} = \sum_{n_a=0}^{\infty} \sum_{n_b=0}^{\infty} \sum_{m=-n_<}^{+n_<} \{[(-1)^{n_b+m}(n_a+n_b)!] \times Q_{n_a}^{m*} Q_{n_b}^{m}\} / \{[(n_a+|m|)!(n_b+|m|)!] \times r_{ab}^{n_a+n_b+1}\} \quad (2)$$

where n_a, n_b are the orders of the multipoles (0 = monopole, 1 = dipole, 2 = quadrupole, *etc.*), $n_<$ is the smaller of n_a and n_b, and $Q_{n_a}^{m*}$ and $Q_{n_b}^{m}$ are the multipole moments expressed as spherical harmonics. The quantities Q_n^m can be calculated from the tensor elements of the various multipole moments in Cartesian

coordinates as follows

$$\begin{aligned} Q_0^0 &= q \\ Q_1^1 &= -(\mu_x - i\mu_y) \\ Q_1^0 &= \mu_z \\ Q_1^{-1} &= \mu_x + i\mu_y \\ Q_2^0 &= 0.5^* Q_{zz} \\ Q_2^1 &= -(Q_{xz} - iQ_{yz}) \\ Q_2^2 &= Q_{xx} - 2iQ_{xy} - Q_{yy}. \end{aligned} \tag{3}$$

The quadrupole tensors are symmetric, so that $Q_{ij} = Q_{ji}$ q is the total charge of the molecule or charge distribution.

Electrostatic energy calculations employing molecular multipole–multipole interactions have several advantages over the various point-charge methods which are most commonly used. One advantage is that the magnitude of the dipole and quadrupole moments can be verified experimentally, whereas condensing the charge distribution calculated from the molecular wavefunctions into a relatively small number of point charges is not an exact procedure, and considerable disagreement exists as to the best methodology. In addition, higher-order multipole interactions fall off much more quickly than the $1/r$ dependence of point-charge interactions and can be calculated by a direct lattice summation. For example, dipole–dipole interactions exhibit an r^{-3} dependence and will converge much faster than a $1/r$ series using even the most efficient Ewald summation techniques. From a sufficient distance, a point dipole will appear neutral, even if the magnitude of its dipole moment is very large. Another advantage is the reduced number of interactions to be considered when using molecular multipoles. For example, each benzene molecule contains a point charge on each of the 12 atoms, but only one molecular quadrupole moment and no dipole or octapole moment.

Most of the electrostatic calculations performed to date on molecular solids such as benzene have been carried out using point charges and here we use the calculations of Williams (1983) as a basis for comparison. One reported concern in using molecular multipoles is the lack of sensitivity to fine structural differences around the principal axes of symmetry, particularly for quadrupole moments, even when cylindrical symmetry is not assumed. For example, it is possible to distinguish the eclipsed and antiparallel configurations of aniline dimers using only the quadrupole moments in (2), but not the eclipsed and staggered configurations of the parallel benzene dimer. The point-charge model, however, is also unable to clearly distinguish the two configurations. Using Williams' point-charge model we obtained an energy difference of only 0.5% between the eclipsed and the staggered dimer. It is important to note that these calculations are based on the electrostatic contribution only and do not include the dispersive nor closed-shell repulsive interactions, for which the difference in energy is considerable between the two configurations.

When the molecular multipole model was applied to a series of closely packed structures of benzene, the herringbone edge-to-face configuration was shown to be more stable than the slipped-stack parallel structure, consistent with the experimental data. Without the electrostatic component, the slipped-stack structure exhibited a lower energy. Even though the electrostatic contribution to the lattice energy cannot be separated experimentally from the total binding energy of the solid, for comparison with our results, the magnitude of the energy we obtained using the molecular multipole model, 2.1 kJ mol^{-1}, was consistent with the results calculated by other methods (Williams, 1969; Evans & Watts, 1976) and the type of packing obtained agreed with experiment. The various models for the charge distributions may predict slightly different crystal structures if electrostatic energy was the sole criteria used, but as the electrostatic contribution to the lattice energy is only a minor part of the total, and is not used in the actual minimization process, it is expected that any error is minimized. Therefore, at the present time the molecular multipole model appears adequate as an efficient screening tool.

To summarize the final stage, each structure is sorted on the basis of the energy obtained from the following expression

$$E = \sum_{ij} 4\varepsilon_{ij}[(\sigma_{ij}/r_{ij})^{12} - (\sigma_{ij}/r_{ij})^6] + E_{coul}, \tag{4}$$

where i is summed over all atoms in the reference molecule and j over all other atoms in neighboring molecules within a 10 Å radius, and E_{coul} is calculated as in (4). As the energy of each closely packed structure is calculated, it is compared with the three best structures within its space group and with the ten best structures overall. These results are then reported.

5. Results

The following molecules were selected for this study: benzene, naphthalene, anthracene, tetracene, pentacene, phenanthrene, pyrene, triphenylene, 1:2:5:6-dibenzanthracene, trindan, perylene, durene, hexane, octane and bicyclohexylidine. The structures of selected molecules are shown in Fig. 1. Table 1 contains the lattice constants and angles of the experimental structure, the *ICE*9 predicted structure corresponding to experiment and the global energy minimum if different from experiment. The energy and packing index for the lowest energy structure in each space group for every molecule is given in Tables 2–18. Space groups such as $P2_1/c$, in which different Z values are possible, are listed separately if the structures in each case are different. For space groups

Table 1. *Lattice parameters for experimental structures (Exp't.), predicted structure (Pred.) closest to the experimental structure (Calc.) and the lowest energy predicted structures*

Molecule/ structure	Space group	Z	a (Å)	b (Å)	c (Å)	α (°)	β (°)	γ (°)
Bicyclohexylidene								
Exp't. (*a*)	$P\bar{1}$	1	5.32	6.25	8.36	72.8	79.1	74.4
Pred.	$P\bar{1}$	1	5.21	6.14	8.74	66.1	90.0	73.8
Hexane								
Exp't. (*b*)	$P\bar{1}$	1	4.17	4.70	8.57	83.4	87.2	75.0
Pred.	$P\bar{1}$	1	4.15	5.05	8.12	83.3	63.7	89.0
Octane								
Exp't. (*b*)	$P\bar{1}$	1	4.16	4.75	11.00	85.2	84.5	105.1
Calc.	$P\bar{1}$	1	4.17	4.75	11.10	90.0	92.2	76.8
Pred.	$P\bar{1}$	1	4.16	5.06	12.49	55.2	69.0	89.4
Benzene								
Exp't. (*c*)	*Pbca*	4	7.39	9.42	6.81	90.0	90.0	90.0
Calc.	*Pbca*	4	7.44	9.36	6.80	90.0	90.0	90.0
Pred.	*Pbca*	4	14.23	5.64	5.64	90.0	90.0	90.0
Durene								
Exp't. (*d*)	$P2_1/a$	2	11.57	5.77	7.03	90.0	66.7	90.0
Calc.	$P2_1/a$	2	11.12	6.01	7.08	90.0	65.9	90.0
Pred.	$P\bar{1}$	1	7.77	6.77	4.14	74.8	88.2	76.6
Perylene								
Exp't. (*e*)	$P2_1/a$	4	11.35	10.87	10.31	90.0	100.8	90.0
Calc.	$P2_1/a$	4	11.64	10.84	10.41	90.0	113.6	90.0
Pred.	$P2_1/c$	4	14.02	4.16	22.07	90.0	100.8	90.0
Naphthalene								
Exp't. (*f*)	$P2_1/a$	2	8.12	5.95	8.64	90.0	124.6	90.0
Calc.	$P2_1/a$	2	8.07	5.83	8.65	90.0	60.3	90.0
Pred.	$P2_1/a$	2	10.26	6.01	5.76	90.0	72.0	90.0
Anthracene								
Exp't. (*g*)	$P2_1/a$	2	8.44	6.00	11.12	90.0	54.4	90.0
Calc.	$P2_1/a$	2	8.42	5.91	11.12	90.0	57.3	90.0
Pred.	$P\bar{1}$	1	3.43	9.81	3.95	80.1	71.2	65.8
Tetracene								
Exp't. (*h*)*	$P\bar{1}$	1	7.98	6.14	13.57	78.7	66.8	87.5
Pred.	$P2_1/c$	4	11.01	4.66	21.78	90.0	87.0	90.0
Pentacene								
Exp't. (*h*)*	$P\bar{1}$	1	7.90	6.06	16.01	78.1	67.4	85.8
Pred.	$P\bar{1}$	1	4.28	6.11	16.34	75.1	54.0	83.0
Phenanthrene								
Exp't. (*i*)	$P2_1$	2	8.46	6.16	9.47	90.0	82.3	90.0
Calc.	$P2_1$	2	8.77	5.96	9.46	90.0	82.8	90.0
Pred.	$P2_1/a$	4	21.13	3.79	13.19	90.0	59.1	90.0
Pyrene								
Exp't. (*j*)	$P2_1/a$	4	13.60	9.24	8.37	90.0	79.8	90.0
Calc.	$P2_1/a$	4	13.48	9.45	8.07	90.0	82.1	90.0
Pred.	$P2_1/c$	4	7.69	8.23	17.70	90.0	61.6	90.0
Triphylene								
Exp't. (*k*)	$P2_12_12_1$	4	13.17	16.73	5.26	90.0	90.0	90.0
Calc.	$P2_12_12_1$	4	12.86	16.58	5.20	90.0	90.0	90.0
Pred.	$P2_1$	2	4.09	14.12	9.95	90.0	78.2	90.0
1:2:5:6-Dibenzanthracene								
Exp't. *A* (*l*)	$P2_1$	2	6.59	7.84	14.17	90.0	76.5	90.0
Calc. *A*	$P2_1$	2	6.40	7.82	14.00	90.0	77.6	90.0
Exp't. *B* (*m*)	*Pcab*	4	8.22	11.39	15.14	90.0	90.0	90.0
Calc. *B*	*Pcab*	4	8.27	11.84	14.67	90.0	90.0	90.0
Pred.	$P2_1$	2	11.17	14.65	4.20	90.0	76.2	90.0
Trindan								
Exp't. (*n*)	$P2_1/c$	4	12.67	5.87	16.92	90.0	68.32	90.0
Calc.	$P2_1/c$	4	13.13	6.18	17.16	90.0	69.29	90.0
Pred.	$P2_1/c$	4	4.14	13.65	19.11	90.0	73.80	90.0

References: (*a*) Boyko & Vaughan (1964); (*b*) Norman & Mathisen (1961*a*, *b*); (*c*) Bacon, Curry & Wilson (1964); (*d*) Robertson (1933); (*e*) Donaldson, Robertson & White (1953); (*f*) Kozin & Kitaigorodsky (1953); (*g*) Mason (1964); (*h*) Campbell, Robertson & Trotter (1962); (*i*) Trotter (1963); (*j*) Robertson & White (1947*a*); (*k*) Ahmed & Trotter (1963); (*l*) Iball & Robertson (1933), Krishnan & Banerjee (1935); Iball (1936); (*m*) Robertson & White (1947*b*); (*n*) Bokyo & Vaughan (1964).

* Note: The asymmetric unit is two half-molecules.

Table 2. *Lowest energy structures (kJ mol^{-1}) in each space group for bicyclohexylidene predicted by ICE9*

Space group	Z	E_{Total}	E_{LJ}	E_{Coul}	Packing index
$P\bar{1}$	1	−115.30	−115.26	−0.04	0.6232
$C2/c$	4	−108.15	−108.15	−0.00	0.6031
$P2_1/c$	4	−106.55	−106.55	−0.04	0.5984
$Pca2_1$	4	−103.87	−103.83	−0.04	0.5872
$Pna2_1$	4	−103.58	−103.54	−0.00	0.5927
$P2_1/c$	2	−101.91	−101.86	−0.04	0.5864
$P2_1$	2	−101.49	−101.45	0.00	0.5857
$P2_12_12_1$	4	−99.39	−99.35	−0.00	0.5839
$Pbca$	4	−85.12	−85.08	−0.00	0.5139

Table 3. *Lowest energy structures (kJ mol^{-1}) in each space group for hexane predicted by ICE9*

Space group	Z	E_{Total}	E_{LJ}	E_{Coul}	Packing index
$P\bar{1}$	1	−75.40	−75.57	0.13	0.5541
$P2_1/c$	4	−74.19	−74.06	0.08	0.5494
$P2_1/c$	2	−74.06	−73.98	−0.08	0.5461
$P2_1$	2	−73.69	−73.81	0.13	0.5460
$Pna2_1$	4	−71.09	−71.05	−0.08	0.5355
$Pca2_1$	4	−70.55	−70.59	0.04	0.5355
$C2/c$	4	−70.55	−70.51	−0.08	0.5334
$P2_12_12_1$	4	−67.91	−68.16	0.25	0.5245
$Pbca$	4	−63.05	−63.01	−0.04	0.5046

which have different settings, *e.g.* $P2_1/a$ is a nonstandard setting of $P2_1/c$, separate listings of these settings are given if different structures were obtained. Graphical projections of several key results are also given. Graphical representations of the results are not shown for all molecules because of space limitations. In general,

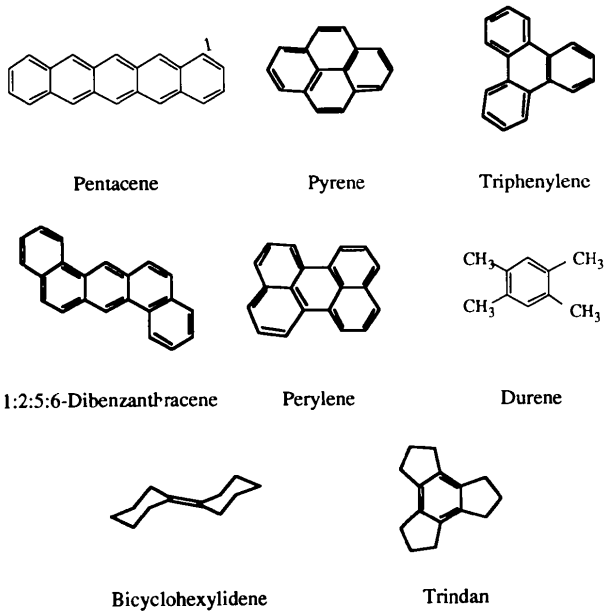

Fig. 1. Selected structures for several molecules used in this study.

Table 4. *Lowest energy structures (kJ mol^{-1}) in each space group for octane predicted by ICE9*

Space group	Z	E_{Total}	E_{LJ}	E_{Coul}	Packing index
$P\bar{1}$	1	−97.89	−98.14	−0.25	0.5807
$P2_1/c$	4	−96.46	−96.30	−0.17	0.5744
$P2_1/c$	2	−95.84	−95.75	−0.08	0.5732
$C2/c$	4	−93.62	−94.12	0.54	0.5708
$P2_1$	2	−93.62	−93.91	0.29	0.5675
$Pca2_1$	4	−92.28	−92.49	0.21	0.5601
$Pna2_1$	4	−92.07	−92.78	0.71	0.5634
$Pbca$	4	−80.55	−80.39	−0.17	0.5266

in these projections H atoms are not shown in order to simplify the representation of the crystal structure.

5.1. *Bicyclohexylidene*

The most unequivocal prediction by *ICE9* of an experimentally observed structure was for bicyclohexylidene, with the observed structure in $P\bar{1}$, Fig. 2(*a*), predicted to be almost 8.37 kJ mol^{-1} lower in energy than the structure in the second most probable space group,

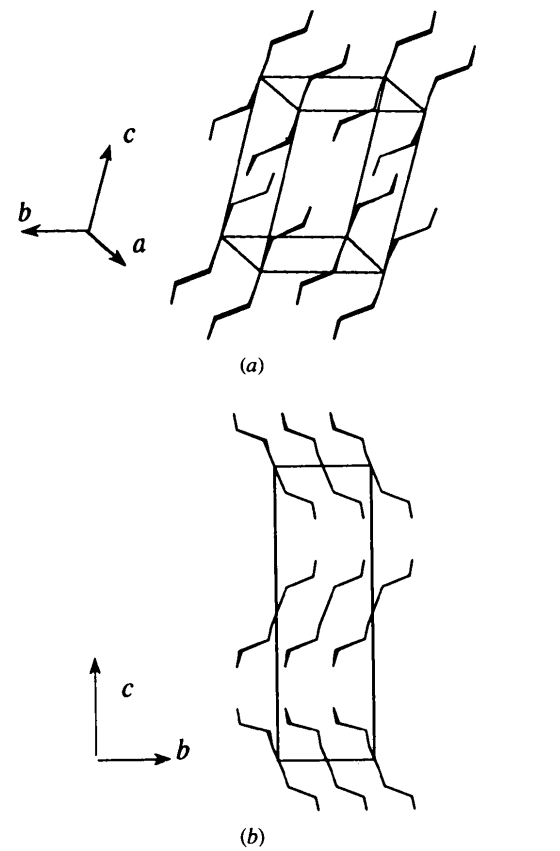

Fig. 2. (*a*) Experimental and predicted structure for bicyclohexylidene in space group $P1$, $Z = 1$. (*b*) Second most probable predicted crystal structure, in $C2/c$, $Z = 14$. The packing within layers is very similar to the observed structure.

Table 5. *Lowest energy structures (kJ mol^{-1}) in each space group for octane predicted by ICE9*

Space group	Z	E_{Total}	E_{LJ}	E_{Coul}	Packing index
Pbca	4	−50.16	−48.19	−1.97	0.5675
$P2_1$	2	−49.99	−47.90	−2.09	0.5646
$P2_1/c$	2	−49.86	−47.86	−1.84	0.5655
$P2_1/c$	4	−49.70	−47.86	−1.84	0.5655
Pna	4	−48.90	−46.93	−1.97	0.5597
$P\bar{1}$	2	−48.86	−47.14	−1.67	0.5652
$P\bar{1}$	1	−48.82	−47.35	−1.47	0.5616
$Pca2_1$	4	−48.61	−46.52	−2.09	0.5450
$C2/c$	4	−48.11	−48.65	−0.54	0.5709
*Pbca**	4	−47.98	−46.47	−1.51	0.5641
Cmcm	4	−47.23	−45.64	−1.59	0.5443
Pnma	4	−45.38	−43.46	−1.93	0.5310
$C2/c$	4	−44.59	−44.00	−0.59	0.5582
Pbcn	4	−43.12	−44.09	−0.96	0.5394
$Pmc2_1$	2	−34.62	−32.70	−1.93	0.4419
Cmcm	4	−28.81	−33.33	4.52	0.4399

* Experimental structure

Table 6. *Energies calculated using PCK83 (kJ mol^{-1})*

Space group	E_{Total}	E_{Coul}
Pbca	−53.00	−9.04
*Pbca**	−52.38	−9.67
$P2_1/c$	−52.13	−7.66
$P2_1$	−52.13	−5.28
$P\bar{1}$	−48.65	−7.20
$Pna2_1$	−47.14	−11.60

* Experimental structure.

$C2/c$ (Fig. 2*b*, Table 2). The electrostatic energy is negligible, as would be expected. The packing index was also dramatically higher than those in any other space group, indicating that the predicted structure was by far the most closely packed. The contours of each molecule align closely with adjacent molecules and the positions of the H atoms are staggered to allow closest packing. The irregular shape of bicyclohexylidene severely limits the possible number of low energy, closely packed structures and is undoubtedly responsible for the unambiguousness of the results.

The packing within layers in the second most probable space group, $C2/c$, is very similar to that within the predicted and experimental structure. The molecules in adjacent layers in $C2/c$, however, are related by a screw axis and hence are angled with respect to each other, in contrast to the observed parallel structure in $P\bar{1}$. All other space groups are clearly eliminated.

5.2. *Saturated linear alkanes: hexane and octane*

For both the saturated linear hydrocarbons hexane and octane, *ICE*9 predicted the correct space group and almost identical crystal structure (Figs. 3*a* and *b*). The structure within layers in the predicted structure is identical to that of the experimental structure, the

Table 7. *Lowest energy structures (kJ mol^{-1}) in each space group for durene predicted by ICE9*

Space group	Z	E_{Total}	E_{LJ}	E_{Coul}	Packing index
$P\bar{1}$	1	−89.64	−89.64	−0.017	0.5653
$P\bar{1}$	1	−83.74	−85.03	1.30	0.5611
$Pca2_1$	4	−83.31	−84.36	1.00	0.5593
Pbca	4	−82.81	−82.73	0.13	0.5526
$P2_1/a$	4	−82.23	−83.11	0.88	0.5591
$P2_1/c$	4	−81.68	−81.81	0.13	0.5494
$Pna2_1$	4	−80.93	−82.19	1.26	0.5501
$P2_1$	2	−80.64	−81.14	0.50	0.5481
$P2_1/a$	2	−80.47	−79.67	−0.80	0.5429
$P2_1/c$	2	−79.76	−80.72	0.96	0.5444
$C2/c$	4	−76.62	−77.20	0.63	0.5330
Pnma	4	−74.44	−74.36	−0.46	0.5248
$C2/c$	4	−73.48	−73.02	−0.46	0.5139
Cmcm	4	−70.88	−70.55	−0.33	0.5114
$Pmc2_1$	2	−69.12	−70.34	1.21	0.5000
Pbcn	4	−64.31	−64.27	−0.04	0.4879
Cmcm	4	−60.62	−60.54	−0.08	0.4705

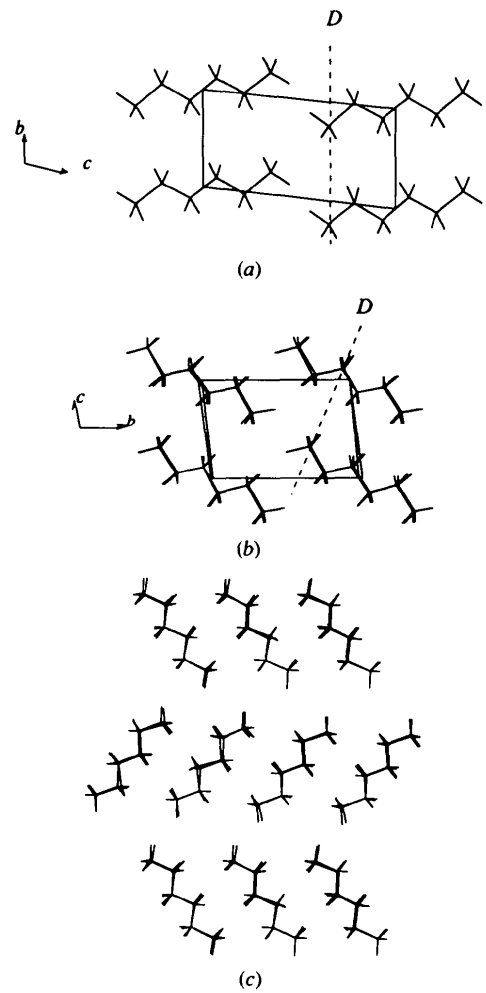

Fig. 3. (*a*) Experimental structure of hexane, space group $P\bar{1}$. (*b*) Structure of the most probable predicted structure, space group $P\bar{1}$. (*c*) Arrangement of the layers in $P2_1/c$, the second most probable predicted space group.

Table 8. *Lowest energy structures (kJ mol^{-1}) in each space group for perylene predicted by ICE9*

Space group	Z	E_{Total}	E_{LJ}	E_{Coul}	Packing index
$P2_1/c$	2	−146.24	−124.93	−21.35	0.6072
$P\bar{1}$	1	−143.57	−122.42	−23.28	0.6026
$P2_1/a$	2	−142.48	−124.31	−18.17	0.6098
$P2_12_12_1$	4	−139.42	−120.33	−19.09	0.5926
Pca	4	−138.75	−117.70	−21.06	0.5811
$P2_1$	2	−136.95	−115.68	−21.23	0.5802
$P2_1/a$	4	−135.59	−115.97	−19.59	0.5847
Pna	4	−134.90	−113.63	−21.23	0.5793
$Pnma$	4	−130.08	−113.17	−16.87	0.5704
$Pbca$	4	−126.90	−119.66	−7.24	0.5818
Pmc	2	−126.65	−104.84	−21.77	0.5285
$C2/c$	4	−117.36	−116.98	−0.38	0.5492
Cmc	4	−113.67	−108.69	−5.02	0.5650
$C2/c$	4	−113.59	−115.26	1.67	0.5703
$Pbcn$	4	−108.44	−108.52	0.08	0.5601
Cmc	4	−90.64	−100.19	9.50	0.5214

Table 9. *Lowest energy structures (kJ mol^{-1}) in each space group for naphthalene predicted by ICE9*

Space group	Z	E_{Total}	E_{LJ}	E_{Coul}	Packing index
$P2_1/a$	2	−73.56	−71.47	−2.05	0.6174
$P2_1/c$	4	−72.85	−69.71	−3.14	0.6002
$P2_1$	2	−72.72	−69.88	−2.85	0.6098
$P2_1/c$	2	−72.68	−69.54	−3.10	0.6056
$P2_12_12_1$	4	−71.59	−68.00	−3.60	0.5970
$Pca2_1$	4	−70.59	−67.16	−3.43	0.6004
$P2_1/a$	4	−70.30	−66.82	−3.48	0.5985
$P\bar{1}$	1	−70.13	−66.53	−3.60	0.5931
$Pna2_1$	4	−69.79	−66.99	−2.81	0.5998
$Pnma$	4	−68.12	−67.45	−0.67	0.6034
$C2/c$	4	−66.32	−63.30	−3.01	0.5814
$Cmcm$	4	−65.23	−63.39	−1.84	0.5913
$Pbca$	4	−63.43	−61.17	−2.26	0.5699
$C2/c$	4	−62.76	−62.17	−0.59	0.5701
$Pbcn$	4	−61.50	−61.25	−2.55	0.5650
$Pmc2_1$	2	−60.88	−55.56	−5.32	0.5166
$Cmcm$	4	−47.56	−47.27	−0.29	0.4727

Table 10. *Lowest energy structures (kJ mol^{-1}) in each space group for anthracene predicted by ICE9*

Space group	Z	E_{Total}	E_{LJ}	E_{Coul}	Packing index
$P\bar{1}$	1	−98.85	−91.40	−7.45	0.6309
$P2_1$	2	−98.22	−90.98	−7.29	0.6363
$P2_1/c$	4	−98.10	−91.02	−7.12	0.6325
$P2_1/a$	2	−98.01	−90.73	−7.29	0.6298
$Pna2_1$	2	−94.79	−88.17	−6.62	0.6211
$C2/c$	4	−94.16	−94.50	−3.52	0.5323
$P2_12_12_1$	4	−93.53	−87.88	−5.65	0.6145
$P2_1/a$	4	−93.16	−89.43	−3.73	0.6277
$Pca2_1$	4	−92.44	−82.94	−9.50	0.5838
$Pbca$	4	−92.24	−94.41	−6.20	0.6138
$Pnma$	4	−90.60	−89.35	−1.26	0.6267
$Pmc2_1$	2	−89.60	−79.55	−10.05	0.5643
$C2/c$	4	−88.01	−82.52	−5.48	0.6084
$Cmcm$	4	−87.46	−80.22	−7.24	0.5839
$Pbcn$	4	−82.56	−80.23	−3.68	0.6010

Table 11. *Lowest energy structures (kJ mol^{-1}) in each space group for tetracene predicted by ICE9*

Space group	Z	E_{Total}	E_{LJ}	E_{Coul}	Packing index
$P2_1/c$	4	−128.03	−116.52	−11.51	0.6506
$P\bar{1}$	1	−127.70	−116.81	−10.89	0.6462
$P2_1/a$	2	−127.36	−113.59	−13.77	0.6450
$P2_1/c$	2	−126.73	−110.41	−16.33	0.6223
$P2_1$	2	−125.35	−110.53	−14.82	0.6244
$P\bar{1}$	2	−124.72	−115.47	−9.25	0.6423
$Pca2_1$	4	−123.51	−107.94	−15.53	0.6047
$Pmc2_1$	2	−120.62	−104.08	−16.50	0.5872
$C2/c$	4	−116.69	−116.94	0.25	0.5978
$Pbca$	4	−119.53	−110.36	−9.00	0.6185
$Cmcm$	4	−114.51	−108.81	−5.69	0.6281
$Pnma$	4	−108.81	−97.55	−11.22	0.5697
$Pbcn$	4	−105.80	−106.34	0.54	0.6182
$Cmcm$	4	−65.44	−96.63	−31.19	0.5462

Table 12. *Lowest energy structures (kJ mol^{-1}) in each space group for pentacene predicted by ICE9*

Space group	Z	E_{Total}	E_{LJ}	E_{Coul}	Packing index
$P\bar{1}$	1	−145.83	−142.90	−2.93	0.5668
$P2_1$	2	−144.53	−141.60	−2.93	0.5659
$P2_1/a$	4	−143.98	−139.59	−4.40	0.5597
$P2_1/a$	4	−142.18	−137.75	−4.48	0.5555
$Pca2_1$	2	−139.17	−137.08	−2.09	0.5472
$Pbca$	4	−139.13	−136.99	−2.14	0.5481
$Pca2_1$	4	−133.94	−132.14	−1.80	0.5493
$Pmc2_1$	2	−133.14	−128.37	−4.77	0.5213
$Pna2_1$	4	−131.42	−127.70	−3.73	0.5307
$C2/c$	4	−131.21	−131.34	0.13	0.5451
$C2/c$	4	−129.92	−129.71	−0.21	0.5460
$Pnmac$	4	−126.48	−127.61	1.13	0.5443
$Cmcm$	4	−125.10	−122.80	−2.34	0.5254
$Pbcn$	4	−122.51	−123.43	0.92	0.5228
$Cmcm$	4	−104.50	−105.21	0.71	0.4715

difference being a slight shift in how the layers are aligned. In the experimental structure the equivalent C atoms in each molecule are in the same plane parallel to the **ab** plane. These planes are almost perpendicular to the **L** axis of the molecules. In the predicted structure, however, the D plane perpendicular to the **L** axis of the molecule passes through the first C atom in one layer and the third C atom in the layer below. Despite the difference in the location of the adjacent layers, the dimensions of the unit cell for the predicted structure are very similar to experiment, 4.15, 5.05, 8.12 and 4.17, 4.70, 8.57 Å, respectively, reflecting the common structures within layers.

In the second most probable space group, $P2_1/c$ with $Z = 4$, the crystal is constructed of layers very similar to the layers in the experimental structure and the center of symmetry of the molecule is maintained. The screw axis and glide plane of the space group $P2_1/c$, however, create differences between the layers. In this space group all the molecules in one layer are rotated 72° about the **L** axis relative to the molecules in the adjacent layers (Fig.

Table 13. *Lowest energy structures (kJ mol^{-1}) in each space group for phenanthrene predicted by ICE9*

Space group	Z	E_{Total}	E_{LJ}	E_{Coul}	Packing index
$P2_1/a$	4	−114.76	−91.10	−23.66	0.6326
$P2_1/c$	4	−111.29	−85.33	−26.00	0.6099
$P2_12_12_1$	4	−110.57	−87.46	−23.11	0.6142
$Pca2_1$	4	−109.36	−83.61	−25.79	0.6040
$P\bar{1}$	2	−110.41	−87.55	−22.90	0.6154
$P2_1$	2	−105.97	−84.15	−21.81	0.6054
$Pna2_1$	4	−104.25	−80.72	−23.53	0.5999
$C2/c$	4	−84.41	−60.46	−23.95	0.4684
$Pbcn$	4	−70.97	−70.09	−0.88	0.5356

Table 14. *Lowest energy structures (kJ mol^{-1}) in each space group for pyrene predicted by ICE9*

Space group	Z	E_{Total}	E_{LJ}	E_{Coul}	Packing index
$P2_1/c$	4	−108.69	−99.23	−9.46	0.6465
$P\bar{1}$	1	−107.89	−98.39	−11.60	0.6304
$P2_1/c$	2	−107.77	−98.05	−9.71	0.6439
$P2_1/a$	4	−107.14	−97.18	−9.96	0.6393
$P2_1$	2	−104.75	−95.54	−9.21	0.6360
$P2_12_12_1$	4	−103.00	−93.03	−9.96	0.6293
$Pca2_1$	4	−102.16	−93.83	−8.33	0.6225
$Pna2_1$	4	−99.65	−90.85	−8.79	0.6151
$C2/c$	4	−96.38	−88.55	−7.83	0.6123
$Pbca$	4	−94.45	−85.96	−8.88	0.5832
$Pnma$	4	−92.15	−87.17	−4.98	0.5898
$Cmcm$	4	−90.60	−85.37	−5.28	0.5986
$C2/c$	4	−82.98	−82.31	−0.67	0.5919
$Pbcn$	4	−81.39	−82.69	−1.30	0.5903
$Pmc2_1$	2	−74.11	−68.12	−5.99	0.4677
$Cmc2_1$	4	−68.79	−65.57	−3.22	0.4664
$Cmcm$	4	−68.66	−65.44	−3.22	0.4733

Table 15. *Lowest energy structures (kJ mol^{-1}) in each space group for triphenylene predicted by ICE9*

Space group	Z	E_{Total}	E_{LJ}	E_{Coul}	Packing index
$P2_1$	2	−130.63	−111.58	−19.05	0.6393
$P2_12_12_1$	4	−130.38	−111.58	−18.80	0.6393
$P\bar{1}$	2	−129.50	−113.25	−16.24	0.6436
$P2_1/c$	4	−128.70	−107.10	−21.60	0.6309
$Pna2_1$	4	−126.19	−114.76	−11.43	0.6511
$Pca2_1$	4	−123.89	−107.52	−16.37	0.6234

Table 16. *Lowest energy structures (kJ mol^{-1}) in each space group for dibenzanthracene predicted by ICE9*

Space group	Z	E_{Total}	E_{LJ}	E_{Coul}	Packing index
$P2_1$	2	−156.21	−139.09	−17.12	0.6208
$P\bar{1}$	1	−155.67	−137.38	−18.34	0.6182
$P2_1/c$	2	−151.02	−139.92	−11.10	0.6244
$P2_1/c$	4	−148.05	−128.91	−19.26	0.6018
$Pca2_1$	4	−145.37	−129.62	−15.74	0.5997
$Pna2_1$	4	−143.69	−123.55	−20.10	0.5851
$C2/c$	4	−142.64	−123.38	−19.26	0.5774
$Pcab$	4	−142.10	−128.37	−13.73	0.5989
$Pbca$	4	−141.93	−128.24	−13.73	0.5988

Table 17. *Lowest energy structures (kJ mol^{-1}) in each space group for trindan predicted by ICE9*

Space group	Z	E_{Total}	E_{LJ}	E_{Coul}	Packing index
$P2_1/c$	4	−114.01	−114.26	0.230	0.4027
$P\bar{1}$	2	−113.76	−113.88	0.121	0.4171
$P2_12_12_1$	4	−112.71	−112.67	−0.662	0.4231
$P2_1/c$	4	−110.87	−111.08	0.214	0.4132
$Pna2_1$	4	−110.07	−110.28	0.218	0.4128
$P2_1$	2	−108.56	−108.77	0.209	0.4071
$Pca2_1$	4	−104.63	−104.59	−0.063	0.4056

Table 18. *Summary of results*

Molecule	Ranking of correct space group	ΔE from E_{global} (kJ mol^{-1})	Experimental structure found?
Benzene	1	2.18	Yes
Naphthalene	1	1.30	Yes
Anthracene	4	0.75	Yes
Tetracene	2	0.67	Close*
Pentacene	1	1.84	Close*
Phenanthrene	6	29.39	Close
Pyrene	1	5.23	Yes
Triphenylene	2	12.14	Yes
1:2:5:6-Dibenza. *A*	1	N.A.	Yes†
1:2:5:6-Dibenza. *B*	7	–	Close
Perylene	1	37.18	Close
Durene	5	8.08	Yes
Hexane	1	3.60	Yes
Octane	1	8.25	Yes
Bicyclohexylidene	1	0	Yes
Trindan	1	28.97	Close

* Predicting the exact structure is not possible for tetracene and pentacene, as the experimental asymmetric unit consists of two half molecules, for which *ICE*9 does not make previsions at this time. The ΔE given for the energy relates to structures which are as close as possible to the experimental structures based on intermolecular angles and separation. † A structure with similar lattice constants was found, but experimental coordinates are not known.

3*c*), in contrast to the experimental and most probable predicted structures in which all the molecules are parallel throughout the structure.

Dovetailing of the H atoms along the entire length of the saturated molecule maximizes the dispersion energy and fills space efficiently, and hence was a dominant characteristic in the layers of all the low-energy structures for hexane and octane. The structure within the layers was the same for the experimental structures and for the predicted structures in $P\bar{1}$ and in $P2_1/c$, the second most probable space group. Other possible configurations of the molecules within layers were clearly eliminated. The weaker interactions between molecules in different layers were not sufficient, however, to give an overwhelming preference to configurations where the molecules making contact across the interface were parallel or angled. It is doubtful that the differences in energy between the two types of structures is resolvable, irrespective of how accurately

one parametrizes an empirical nonbonded interaction potential between saturated hydrocarbons.

For all the saturated compounds, electrostatic interactions were negligible, as expected, and did not influence the ranking of the predicted structures. It is also worthy of note that although the Lennard–Jones parameters were developed using only aromatic hydrocarbons, the lattice constants obtained for the saturated alkanes were very close to the experimental values. In the case of octane, for example, the observed lattice dimensions are 4.16, 4.75 and 11.00 Å, and *ICE*9 identified a minimum with lattice constants 4.166, 4.755 and 11.105 Å.

5.3. *General results for planar aromatic hydrocarbons*

There are several general types of stacked and herringbone packing structures which are possible for the planar aromatic hydrocarbons (Fig. 4). The possibilities are not as limited as for bicyclohexylidene, hexane and octane. The lack of protrusions, bumps and hollows on the aromatic molecules allows for many more degrees of freedom than the mostly saturated hydrocarbons and hence many more ways to achieve close-packing and a low van der Waals' energy. The greater number of degrees of freedom for planar aromatic molecules results in a larger number of structures in a wide variety of space groups with an energy near the global minimum. Within these varied structures, however, many common features were observed. The smaller molecules, such as benzene, naphthalene, anthracene and phenanthrene, can achieve close packing and hence a low energy with a Type I edge-to-face herringbone structure as in Fig. 4. This type of packing was predicted correctly for benzene and naphthalene. For anthracene, a slipped-stack structure was predicted to be slightly lower, 0.15 kJ mol^{-1}, than the observed herringbone type of packing. The larger molecules, such as pyrene and perylene, could not fill space if they were arranged entirely edge-to-face (type I) and hence are observed to be constructed of dimers or rows of parallel molecules which are then angled to neighboring dimers or rows (types IV and V). The experimentally observed type of packing was predicted to be the most probable for phenanthrene, pyrene and triphenylene. For tetracene, pentacene and durene the correct packing type was close in energy to the global minimum and hence would be considered a highly probable structure.

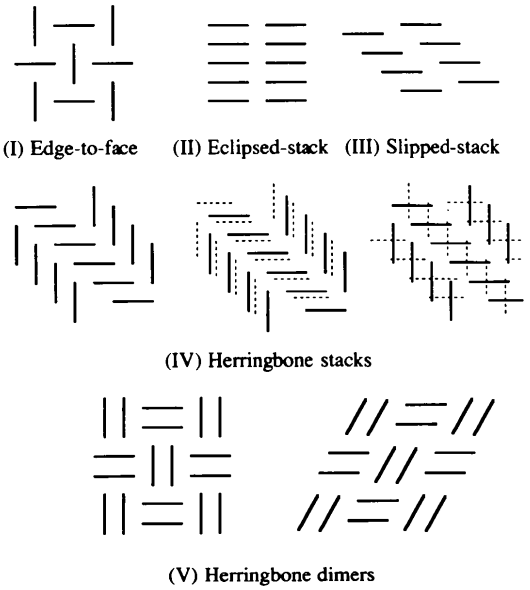

Fig. 4. Types of packing possible for planar aromatic hydrocarbons.

5.4. *Benzene*

Benzene is the model compound most extensively used for the development of packing programs in the literature and hence warrants a more detailed discussion to facilitate comparisons between methods. Benzene crystallizes in a type I configuration in space group *Pbca*, $Z = 4$, in which the molecules are arranged in an edge-to-face manner at 87° angles (Bacon, Curry & Wilson, 1964). This structure was one of the ten lowest energy structures located by *ICE*9, with the lattice constants differing only by 0.05, −0.06 and −0.01 Å from the observed structure. These ten structures, in eight different space groups, were very close in energy, *i.e.* within 2.18 kJ mol^{-1} of the global minimum (Table 5). All but two exhibited an edge-to-face configuration. The global minimum is also in *Pbca*, $Z = 4$, differing primarily from the experimental structure in that the principal axes of the molecules are inclined at approximately 53° within layers in the predicted structure, compared with the 87° mentioned above (Fig. 5). The calculated electrostatic energy and Lennard–Jones energy were both slightly lower than the experimental structure, −1.51 *versus* −1.97 kJ mol^{-1} and −46.47 *versus* −48.19 kJ mol^{-1}, respectively. Comparing the energies of these structures using Williams' program *PCK*83 resulted in the same conclusion, *i.e.* the global minimum located by *ICE*9 in *Pbca* was found to be lower in energy than the experimental structure, although by only 0.63 kJ mol^{-1}.

The electrostatic energies of the ten lowest energy structures fell within the narrow range −1.47 to −2.09 kJ mol^{-1}, with the exception of *C*2/*c* with an electrostatic energy of +0.54 kJ mol^{-1}. The slipped-stack configuration in $P\bar{1}$ possessed a negative electrostatic energy of −1.67 kJ mol^{-1}, as low as or lower than many of the herringbone structures.

The overall results obtained for benzene were also compared with those calculated using Williams' program *PCK*83. *PCK*83 obtained good values for the lattice constants for the experimental structure, the differences being 0.03, −0.12 and 0.18 Å. These results were obtained using the experimental structure as the starting

point for the calculation. In addition, calculations using *PCK*83 were also performed using several different starting positions distributed among several space groups and the lowest energy results obtained from each group are shown in Table 6. *PCK*83 and *ICE*9 both found structures within the experimental space group which were lower in energy than the observed structure, but not by much. Although the search of possible structures using *PCK*83 was hardly exhaustive, the results obtained were similar to those using *ICE*9 in that many structures in different space groups were found to be close in energy to the global minimum. Williams' method, which yields a much greater electrostatic contribution to the lattice energy, did not give a significantly different ordering of the space groups. In addition, local minima were found in space groups $P2_1$ and $P2_1/c$ with energies comparable to the experimental structure in *Pbca*. The thorough search algorithm of *ICE*9 has yielded the first report of slipstacked benzene crystal structures with negative electrostatic components of the energy. Using these structures as starting points for Williams' program, *PCK*83 also produced several slipped-stack structures in $P\bar{1}$ with large negative electrostatic energies comparable to the experimental and other edge-to-face herringbone structures. Williams justified the use of large partial charges on hydrogen and carbon as necessary to reproduce the herringbone configuration. This justification was demonstrated in the gas phase with benzene dimers, but Williams did not examine parallel slipped-stack configurations in the solid for possible structures which, as we have found, can also have large negative electrostatic energies. Hence, the results obtained using Williams' 6-exp-1 potential do not differ significantly from those calculated using the 6–12 plus molecular multipole potential in *ICE*9, yet our method is many orders of magnitude faster.

Both *ICE*9 and *PCK*83 were parametrized for aromatic hydrocarbons and can produce a minimum energy configuration for benzene which is essentially indistinguishable from the experimental structure. That neither *ICE*9 nor *PCK*83 predicted the structure to be the global energy minimum is due to the inherent limitations of empirical pair potentials and not parametrization.

5.5. *Durene*

Our results for durene underscore the principle that ranking probable structures only by the packing index or minimum volume is not always consistent with the ranking from van der Waals' pair potentials, let alone observed structures. Experimentally, durene crystallizes in a herringbone structure in which each molecule is surrounded by almost perpendicular nearest neighbors (Fig. 6). In this way the structure resembles that of

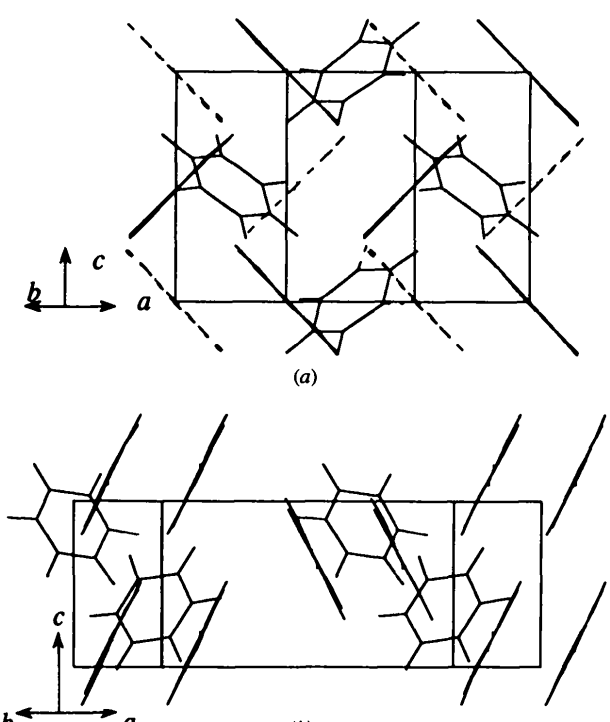

Fig. 5. (*a*) Projection along the molecular edge of benzene in the experimentally observed crystal structure. The bottom layer is indicated by dashed lines. (*b*) Projection along the molecular edge in the predicted global minimum energy structure in space group *Pbca*.

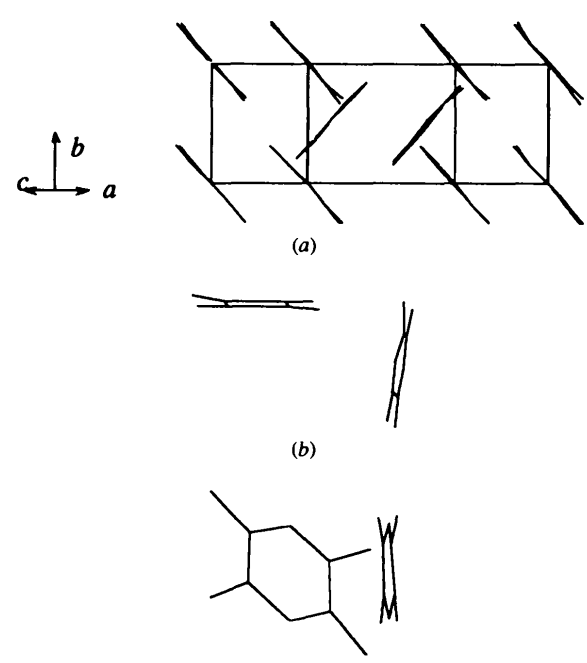

Fig. 6. (*a*) Experimental structure of durene in space group $P2_1/a, Z = 2$, projected along the molecular edge. (*b*) and (*c*) Relative orientations of the two molecules in the unit cell in the observed structure, showing the nearly perpendicular orientation and the *ortho* dovetailing of the methyl groups.

benzene, but with a significant difference. In benzene, the molecules are arranged so that the H atoms on the edge of one molecule are placed at the center of the aromatic face of the other, maximizing the electrostatic interaction. In the durene structure, however, the methyl groups on different molecules interact with each other, rather than with the relatively negative center of the aromatic ring.

The lowest energy structure found by *ICE*9 consists entirely of parallel molecules in a slipped-stack configuration in $P\bar{1}$ (Fig. 7). The stacking structure is such that the methyl groups are staggered along the **L** axis of the molecule. This structure, in which the methyl groups of molecules in one layer are over the aromatic H atoms in the next layer, minimizes the steric interactions between the bulky methyl groups and allows the molecular planes to approach as close as possible, thus maximizing the dispersion energy. In the experimental structure the closest intermolecular contact occurs where the methyl groups are *ortho* to each other and cannot dovetail as effectively, resulting in a somewhat more open structure with a packing index of 0.5324 compared with 0.5653 for the predicted slipped-stack structure. In other words, the experimentally observed structure was far from being closest-packed when compared with other structures obtained using Lennard–Jones pair potentials. These results for durene indicate that caution should be exercised when using close-packing or minimum volume as a sole criterium for selection of structures for more detailed analysis. Even so, *ICE*9 did locate a minimum corresponding to the experimental structure, but with an overall energy of $-77.37\,\mathrm{kJ\,mol^{-1}}$, compared with the global energy minimum at $-85.45\,\mathrm{kJ\,mol^{-1}}$. The electrostatic energy calculated for the observed structure is $-0.55\,\mathrm{kJ\,mol^{-1}}$.

In the second most probable structure, also in $P\bar{1}$, the molecules are arranged so that the methyl groups are staggered on the *ortho* side, similar to the experimental structure but with parallel instead of perpendicular molecular planes (Fig. 8). Because of this arrangement of the relatively bulky methyl groups, the molecular faces cannot approach as closely as in the lowest energy structure and the Lennard–Jones energy is higher and the packing index is lower. The electrostatic energy for this structure is positive, but small ($1.26\,\mathrm{kJ\,mol^{-1}}$).

A herringbone packing similar to the observed structure was the lowest energy configuration determined in the next most probable space group after $P\bar{1}$, $Pca2_1$.

5.6. *Perylene*

The results for perylene exemplify those obtained for the remaining polynuclear aromatic hydrocarbons and hence warrant a detailed discussion. The experimental structure of perylene is composed of parallel pairs of molecules in the configuration shown in Fig. 9, in space group $P2_1/a$, $Z = 4$. Within one layer these pairs of molecules are arranged in an edge-to-face herringbone manner with respect to the surrounding pairs. Across these layers, the pairs are arranged in an extended edge-to-edge stack of parallel molecules. *ICE*9 located a minimum corresponding to the observed structure, but with a somewhat higher energy and lower packing index than the global minimum.

The lowest energy structure found by *ICE*9 was also in space group $P2_1/c$ (Fig. 10), but in a different orientation

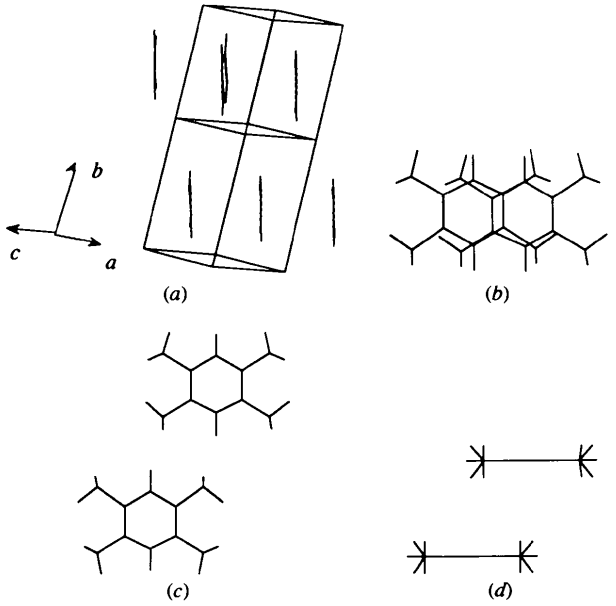

Fig. 7. (*a*) The predicted lowest energy structure of durene in space group $P\bar{1}$, shown in projection along the molecular edge. (*b*) Interlocking methyl groups in the molecular plane, and (*c*) and (*d*) in the stacking of adjacent planes. H atoms are indicated.

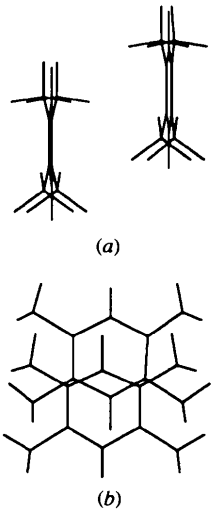

Fig. 8. The second lowest energy structure predicted for durene by *ICE*9 in space group $P\bar{1}$, showing a different close-packing arrangement from that in the lowest energy structure in Fig. 8. (*a*) View parallel to the molecular plane; (*b*) view perpendicular to the molecular plane.

than the experimental structure. The relationship between molecules in the predicted structure is similar to that observed, except that rather than being composed of pairs of parallel molecules it is composed of extended rows of parallel molecules within the layer, which are angled to form an edge-to-face arrangement with the adjacent rows. In the experimental structure the parallel molecules are eclipsed by 1.2 Å more than in the predicted structure. Across the layers, the same type of edge-to-edge arrangement is observed in the predicted structure as in the experimental structure.

The second most probable structure also occurred in space group $P2_1/c$, but with $Z = 4$ (Fig. 11). The structure within layers is essentially identical to that of the lowest energy structure, but the layers are oriented such that the molecules within adjacent layers are arranged in a herringbone fashion (at an angle of 75°), rather than parallel. The overall energy of these two structures is very close. The second structure has a slightly lower electrostatic energy than the first (−5.56 compared with −5.10, respectively), but it has a higher Lennard–Jones energy.

The third most probable structure, in space group $P\bar{1}$, $Z = 1$ (Fig. 12), is constructed entirely of the same type of parallel stacking seen in the first two predicted structures. The electrostatic energy of this entirely

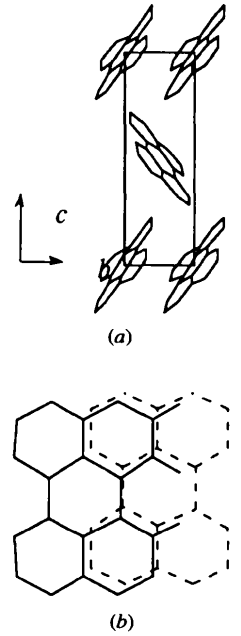

Fig. 10. Most probable structure of perylene predicted by the program, space group $P2_1/c$, $Z = 2$. (*a*) Projection along the *a* axis; (*b*) pair of adjacent perylene molecules showing relative displacement in stacks.

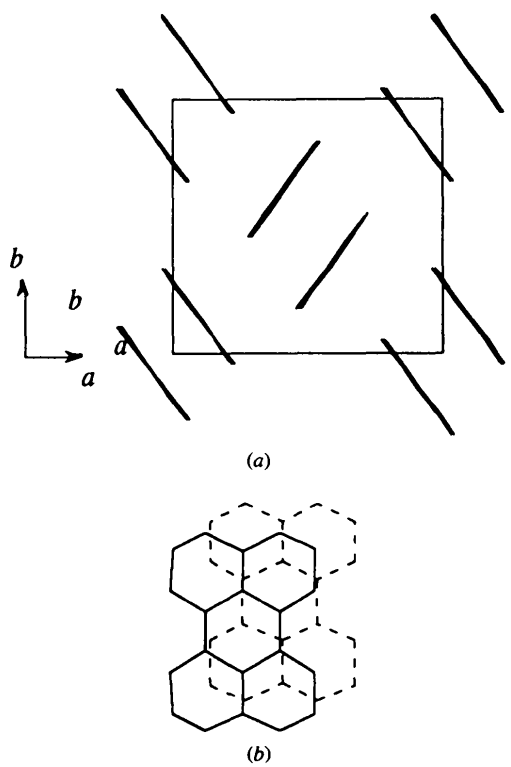

Fig. 9. Experimental structure of perylene, space group $P2_1/a$. (*a*) Projection along the *c* axis; (*b*) relative displacement exhibited in dimers.

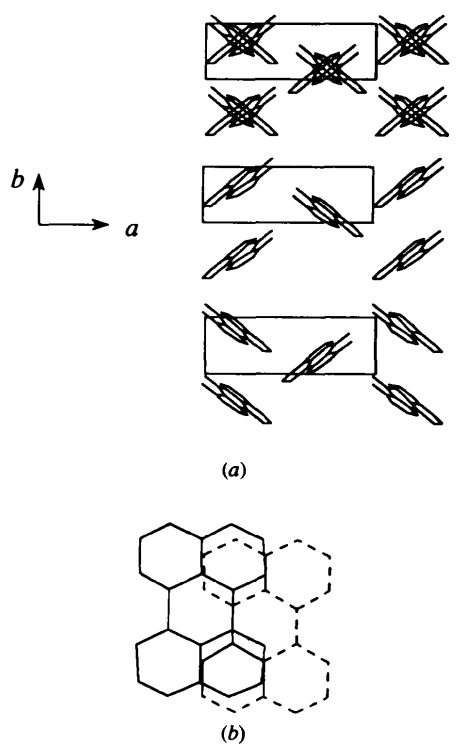

Fig. 11. Second most probable configuration in space group $P2_1/c$, $Z = 4$, predicted by the program for perylene. (*a*) Projection along the *a* axis; (*b*) projection along the *b* axis; (*c*) projection along the *c* axis showing projection of layers together and separately; (*d*) general view.

parallel structure is only 0.42 kJ mol^{-1} higher than the lowest energy structure composed of edge-to-face layers.

The large number of predicted structures very close in energy to the global minimum for perylene illustrates the greater degree of orientational freedom exhibited by these planar aromatic hydrocarbons. The relative displacement of two adjacent coplanar molecules in the experimental structure, as well as the two most probable space groups are shown in Figs. 9(*b*)–11(*b*). The energies of all four crystal structures are very close at this level of approximation and are difficult to resolve through parametrization of empirical potentials, and will probably require more sophisticated quantum mechanical treatment.

6. Summary of results

*ICE*9 found an energy minimum corresponding to the experimental structure for ten of the 16 molecules studied and one very close to experiment for the other six, validating the accuracy of the Lennard–Jones parameters and justifying their use as the sole minimization criteria in *ICE*9 (Tables 1 and 18). In phenanthrene, dibenzanthracene B, pyrene and trindan, in which the experimental structures were not reproduced exactly despite having lattice constants which were close, the molecular orientations deviated by small amounts in the angles of inclination with respect to each other and hence are accessible from the same local minimum. It should also be noted that the parametrization was based on structures at 78 K and the experimental data is often taken at much higher temperatures. This variation in temperature can account for some of the energy and structural differences in Tables 1 and 18.

The location of all the experimental structures but one demonstrates how effectively and thoroughly this method evaluates the extremely large search space of organic molecular crystals. Our results show that the number of possible structures with energy close to the global minimum correlates strongly with the shape of the molecule. Simple regular shapes, such as the planar aromatic hydrocarbons, generate many more reasonable possibilities than the irregularly shaped molecules such as bicyclohexylidine. The correct space group was predicted to be the most probable for ten of the 15 molecules and second most probable for two of them. Many unfavorable space groups were clearly eliminated. Groups containing mirror planes, such as $Pmc2_1$ and *Cmcm*, were found to have the lowest packing indices and the highest energy, and hence the lowest probability of all structures in the cases where they were considered.

The packing indices for the lowest energy structures were found to lie within the fairly narrow range 0.5541–0.6506, with one exception. Trindan's trifold symmetry and protruding H atoms contributed to a very low packing index of 0.4207.

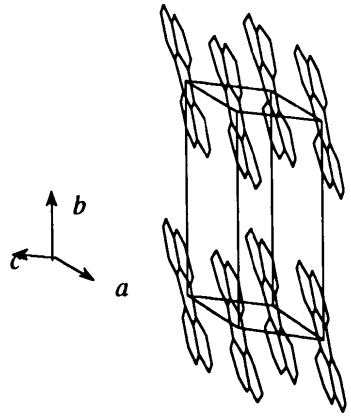

Fig. 12. Third most probable space group $P\bar{1}$, predicted by the program for perylene.

7. Concluding remarks

Our method is general, systematic and can be easily extended to any organic molecular system to generate a set of highly probable crystal structures in a short period of time, using any reasonable set of Lennard–Jones parameters. We have found van der Waals' pair potentials to be an efficient method for the close-packing of organic molecules and very effective as a rough approximation with broad applications. For saturated or mostly saturated hydrocarbons, such as those investigated in this work, *ICE*9 provides good results without extensive additional refinements in the energy calculations of the predicted lowest energy van der Waals' structures, *i.e.* in solids where shape plays a strong role and complicated electronic effects are minimal. Molecular polarity and the resultant electrostatic contribution to the lattice energy can be successfully approximated using the molecular multipole model. For the planar aromatic hydrocarbons, empirical Lennard–Jones parameters plus molecular multipole moments are required to give good approximations and were able to locate minima corresponding to the experimental structures, but are too limited to distinguish the actual structure from a number of possibilities on the basis of energy calculations at this level alone. Further refinement of the energy with more sophisticated methods would be necessary for these materials to arrive at an unequivocal prediction.

Having a technique which can thoroughly examine an extremely large search space for reasonable structural possibilities has provided a framework in which to evaluate empirical methods for obtaining the nonbonded energy. Although considerable work has been carried out on the benzene dimer and clusters over the years, until now no one has reported that an electrostatic potential based on point charges, bond dipoles or molecular

multipole moments can yield a parallel slipped-stack structure for crystalline benzene which has a larger negative electrostatic component than does the experimental herringbone structure.

van der Waals' interactions are often thought of as being very simple to describe and on a certain level that is true. Yet, the inability to clearly distinguish the experimental structure in all cases in this study is a limitation of empirical pair parameters in general and not due to inadequate parameters or electrostatic models. We need to do more than merely add electrostatic potentials on top of van der Waals' pair potentials to obtain results accurate enough to distinguish the experimental structures from a number of reasonable possibilities on the basis of energy, particularly for planar aromatic molecules. This is probably even more true for polar molecules containing heteroatoms. The assumption of independent transferable pair potentials ignores the possibility of multibody effects and polarization of intermediate bodies, as well as differences in the same type of atom from molecule to molecule. Empirical potentials, even ones accurately calculated at a high level of theory, do not take into account how that potential can change due to polarization of the molecule in the crystal environment. In addition, the separation of the energy of molecular solids into dispersion, repulsion and electrostatic contributions is but an artificial construct for simplicity and expediency. To decribe the intermolecular interactions accurately in molecular solids is actually very complicated and requires the most advanced quantum mechanical methods which are available today.

The authors would like to thank The Ohio Supercomputer Center for their generous support as well as the NASA Graduate Student Researchers Fellowship Program for their guidance and support.

References

Ahmed, F. R. & Trotter, J. (1963). *Acta Cryst.* **16**, 503–508.
Bacon, G. E., Curry, N. A. & Wilson, S. A. (1964). *Proc. R. Soc. London Ser. A*, **279**, 98–110.
Boden, N., Davis, P. P., Stam, C. H. & Wesselink, G. A. (1973). *Mol. Phys.* **25**, 81–86.
Bondi, A. (1968). *Mol. Cryst.* **3**, 479–492.
Boyko, E. R. & Vaughan, P. A. (1964). *Acta Cryst.* **17**, 152–158.
Buckingham, A. D. & Fowler, P. W. (1983). *J. Chem. Phys.* **79**, 6426–6428.
Buckingham, A. D. & Fowler, P. W. (1985). *Can. J. Chem.* **63**, 2018–2025.
Campbell, R. B., Robertson, J. M. & Trotter, J. (1962). *Acta Cryst.* **15**, 289–290.
Chemla, D. S. & Zyss, J. (1987). Editors. *Nonlinear Optical Properties of Organic Molecules and Crystals.* New York: Academic Press.
CHEM-X. Chemical Design, Ltd, Oxford, England (1990).
Cox, E. G., Cruickshank, D. W. J. & Smith, J. A. S. (1958). *Proc. R. Soc. Ser. A*, **247**, 1–21.
Donaldson, D. M., Robertson, J. M. & White, J. G. (1953). *Proc. R. Soc. Ser. A*, **220**, 311–321.
Evans, D. J. & Watts, R. O. (1976). *Mol. Phys.* **1**(31), 83–96.
Frisch, M. J., Head-Gordon, M., Trucks, G. W., Foresman, J. B., Schlegel, H. B., Raghavachari, K., Robb, M., Binkley, J. S., Gonzales, C., Defrees, D. J., Fox, D. J., Whiteside, R. A., Seeger, R., Melius, C. F., Baker, J., Martin, R. L., Kahn, L. R., Stewart, J. J. P., Topiol, S. & Pople, J. A. (1990). *Gaussian*90. Revision H. Pittsburgh, PA: Gaussian, Inc.
Gavezzotti, A. (1989). *J. Am. Chem. Soc.* **111**, 1835–1843.
Gavezzotti, A. (1990). *J. Phys. Chem.* **94**, 4319–4325.
Gavezzotti, A. (1991). *J. Am. Chem. Soc.* **113**, 4622–4629.
Gavezzotti, A. & Desiraju, G. R. (1988). *Acta Cryst.* B**44**, 427–434.
Gdanitz, R. J. (1992). *Chem. Phys. Lett.* **190**, 391–396.
Hall, D. & Williams, D. E. (1975). *Acta Cryst.* A**31**, 56–58.
Hirshfeld, F. L. & Mirsky, K. (1979). *Acta Cryst.* A**35**, 366–370.
Hirshfelder, J. O., Curtiss, C. F. & Bird, R. B. (1954). *Molecular Theory of Gases and Liquids.* New York: John Wiley & Sons, Inc.
Hoffman, B. M., Marinsen, J., Pace, L. J. & Ibers, J. A. (1983). *Extended Linear Chain Compounds*, edited by J. S. Miller, Vol. 3, pp. 459–549. New York: Plenum Press.
Holden, J. R., Du, Z. & Ammon, H. L. (1993). *J. Comp. Chem.* **14**, 422–437.
Iball, J. (1936). *Nature*, **137**, 361.
Iball, J. & Robertson, J. M. (1933). *Nature*, **132**, 750.
Jackson, J. D. (1962). *Classical Electrodynamics.* New York: John Wiley & Sons.
Jeziorski, B., Moszynski, R. & Szalewicz, K. (1994). *Int. J. Quantum Chem.* Quantum Symposium, **28**, oral presentation.
Karfunkel, H. R. & Gdanitz, R. J. (1992). *J. Comp. Chem.* **13**, 1171–1183.
Kirkpatrick, S., Gelatt Jr, C. D. & Vecchi, M. P. (1983). *Science*, **220**, 671–680.
Kitaigorodsky, A. I. (1961). *Organic Chemistry Crystallography.* New York: Consultants Bureau.
Kitaigorodsky, A. I. (1973). *Molecular Crystals and Molecules.* New York: Academic Press.
Kozin, V. M. & Kitaigorodsky, A. I. (1953). *Z. Fiz. Khim. SSSR*, **27**, 534–541.
Krishnan, K. S. & Banerjee, K. (1935). *Z. Krist.* **91**, 170–173.
Mason, R. (1964). *Acta Cryst.* **17**, 547–555.
Mighell, A. D., Himes, V. L. & Rodgers, J. R. (1983), *Acta Cryst.* A**39**, 737–740.
Miller, J. S., Epstein, A. & Reiff, W. M. (1983). *Acc. Chem. Res.* **21**, 114–120.
Norman, N. & Mathisen, H. (1961*a*). *Acta Chem. Scand.* **15**, 1747–1754.
Norman, N. & Mathisen, H. (1961*b*). *Acta Chem. Scand.* **15**, 1755–1760.
Oikawa, S., Tsuda, M., Kato, H. & Urabe, T. (1985). *Acta Cryst.* B**41**, 437–445.
Price, S. L. (1986). *Acta Cryst.* B**42**, 388–401.
Roberts, G. G. (1983). *Sens. Actuators*, **4**, 131–145.
Robertson, J. M. (1933). *Proc. R. Soc. Ser. A*, **141**, 594–602.
Robertson, J. M. & White, J. G. (1947*a*). *J. Chem. Soc.* pp. 358–368.

Robertson, J. M. & White, J. G. (1947*b*). *J. Chem. Soc.* pp. 1001–1010.
Rosenbluth, N., Rosenbluth, A. W., Teller, M. N. & Teller, E. (1953). *J. Chem. Phys.* **21**, 1087–1092.
Rybak, S., Jeziorski, B. & Szalewicz, K. (1991). *J. Chem. Phys.* **95**, 6576–6601.
Rybak, S., Szalewicz, K., Jeziorski, B. & Jaszunski, M. (1987). *J. Chem. Phys.* **86**, 5652–5659.
Shi, X. & Bartell, L. S. (1988). *J. Phys. Chem.* **92**, 5667–5673.
Stone, A. J. (1981). *Chem. Phys. Lett.* **83**(2), 233–239.
Sugi, M. (1985). *J. Mol. Elect.* **1**, 3–17.
Szalewicz, K. & Jeziorski, B. (1979). *Mol. Phys.* **38**, 191–208.
Taylor, R. & Kennard, O. (1984). *Acc. Chem. Res.* **17**, 320–326.
Trotter, J. (1963). *Acta Cryst.* **16**, 605–609.
Waal, B. W. van de (1981). *Acta Cryst.* A**37**, 762–764.
Williams, D. E. (1969). *Acta Cryst.* A**25**, 464–470.
Williams, D. E. (1974). *Acta Cryst.* A**30**, 71–74.
Williams, D. E. (1980). *Acta Cryst.* A**36**, 715–723.
Williams, D. E. (1983). Quantum Chemistry Program Exchange, No. 41.
Williams, D. E. & Starr, T. L. (1977). *Comput. Chem.* **1**, 173–177.
Williams, D. J. (1984). *Angew. Chem. Int. Ed. Engl.* **23**, 690–703.